Enhanced correlation of received power-signal fluctuations in bidirectional optical links



2013 J. Opt. 15 022401

(http://iopscience.iop.org/2040-8986/15/2/022401)

IOP FTC
IOP PUBLISHING JOURNAL OF OPTICS
J. Opt. **15** (2013) 022401 (8pp) doi:10.1088/2040-8978/15/2/022401

FAST TRACK COMMUNICATION

# Enhanced correlation of received power-signal fluctuations in bidirectional optical links

**Jean Minet**[1], **Mikhail A Vorontsov**[1,2], **Ernst Polnau**[1] **and Daniel Dolfi**[3]

[1] Intelligent Optics Laboratory, School of Engineering, University of Dayton, 300 College Park, Dayton, OH 45469-2951, USA
[2] Optonicus, 711 East Monument Avenue, Suite 101, Dayton, OH 45402, USA
[3] Thales Research and Technology—France, RD128, F-91767 Palaiseau Cedex, France

E-mail: mvorontsov1@udayton.edu

Received 23 October 2012, accepted for publication 14 December 2012
Published 10 January 2013
Online at stacks.iop.org/JOpt/15/022401

**Abstract**
A study of the correlation between the power signals received at both ends of bidirectional free-space optical links is presented. By use of the quasi-optical approximation, we show that an ideal (theoretically 100%) power-signal correlation can be achieved in optical links with specially designed monostatic transceivers based on single-mode fiber collimators. The theoretical prediction of enhanced correlation is supported both by experiments conducted over a 7 km atmospheric path and wave optics numerical analysis of the corresponding bidirectional optical link. In the numerical simulations, we also compare correlation properties of received power signals for different atmospheric conditions and for optical links with monostatic and bistatic geometries based on single-mode fiber collimator and on power-in-the-bucket transceiver types. Applications of the observed phenomena for signal fading mitigation and turbulence-enhanced communication link security in free-space laser communication links are discussed.

**Keywords:** atmospheric turbulence, free-space optical communications, fiber optics, optical reciprocity

(Some figures may appear in colour only in the online journal)

## 1. Introduction

The relation between two waves propagating in opposite directions—the so-called bidirectional or counter-propagation—through a common path in an optically inhomogeneous medium such as the turbulent atmosphere has been the subject of numerous studies [1–3]. In most commonly considered double-pass and target-in-the-loop scenarios, a transmitted optical wave propagates through the atmosphere towards a remote object (target) and then propagates back after being scattered off the object's surface [3, 4]. The double-pass propagation results in several interesting effects, including enhanced intensity and phase fluctuations of the backscattered (target-return) wave [1, 5]. In the optical wave propagation geometry that is typical of point-to-point free-space laser communication applications, the counter-propagating waves are generated by two independent monostatic laser transceivers at each end of the communication link. According to the optical reciprocity principle for small size (point source) transceivers, propagation through the same refractive index inhomogeneities results in strong (theoretically 100%) correlation between the power signals measured at opposite ends of the propagation path [6].

 

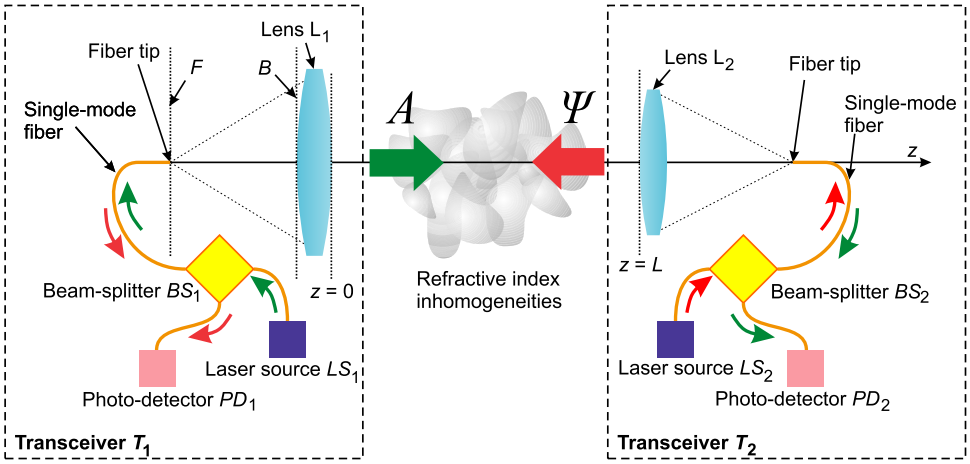


**Figure 1.** Notional schematic of the bidirectional wave propagation link based on single-mode fiber collimator transceivers $T_1$ and $T_2$ composed of collimating lenses $L_1$ and $L_2$ with fiber tips located in their focus and an optical train based on single-mode fiber for both transmitted and received waves.

In this study, we demonstrate through theoretical analysis, supporting numerical simulations and atmospheric experiments that strong correlation between received signals can be also achieved in more realistic cases of finite aperture size monostatic laser transceivers. As shown in section 2, an ideal correlation of received signals at both ends of the propagation path can be observed in an optical link based on specially designed laser transceivers composed of single-mode fiber collimators (SMFC). In the link based on SMFC transceivers, the power received by each transceiver is proportional to the overlapping integral between the counter-propagating waves (also known as the interference metric [7, 8]). The ideal correlation between received power signals that are measured at both ends of the propagation path follows from the derived overlapping integral conservation law. The analytical results obtained in section 2 are verified through numerical simulations and direct experimental measurements of received power signals which are performed over a 7 km-long atmospheric link. The experimental measurements are described in section 3. In section 4, numerical simulations are used to analyze the received signal correlation properties for different transceiver configurations. Potential applications of the observed phenomena in laser communications are discussed in section 5.

## 2. Bidirectional optical link based on SMFC transceivers: mathematical model and analysis

Consider the bidirectional optical propagation setting based on SMFC transceivers $T_1$ and $T_2$ in figure 1. Each SMFC transceiver represents a fiber collimator which is utilized to simultaneously transmit a quasi-monochromatic continuous wave laser beam and receive the corresponding counter-propagating optical wave. Laser beams enter the fiber collimator through the tips of single-mode fibers which are positioned at the collimating lens focus. The outgoing beams propagate through an optically inhomogeneous medium such as the atmosphere and enter the SMFC apertures as illustrated in figure 1. The received optical waves are then focused by the collimating lenses and coupled into the fiber tips. The coupled waves propagate through the single-mode fibers and after passing the fiber-integrated beam splitters $BS_1$ and $BS_2$ enter the photo-detectors $PD_1$ and $PD_2$. These beam splitters are used to separate outgoing and received optical waves. The photo-detectors measure the signals $P_1(t)$ and $P_2(t)$, which are proportional to the powers coupled into the fibers, where $t$ is the time variable and temporal fluctuations of the received signals are caused by random refractive index variations along the propagation path.

Assuming that received signals $P_1(t)$ and $P_2(t)$ can be considered as stationary random processes, we can define the normalized cross-correlation function $\gamma_{12}(\tau)$ as [9]

$$\gamma_{12}(\tau) = \frac{\langle P_1(t)P_2(t+\tau)\rangle - \langle P_1(t)\rangle\langle P_2(t)\rangle}{\left[\langle P_1^2(t)\rangle - \langle P_1(t)\rangle^2\right]^{1/2}\left[\langle P_2^2(t)\rangle - \langle P_2(t)\rangle^2\right]^{1/2}}, \tag{1}$$

where $\langle\cdot\rangle$ denotes averaging over ensemble realizations of random functions $P_1(t)$ and $P_2(t)$. In practice, the ensemble averaging can be replaced by averaging over a sufficiently long time $T \gg \tau_n$, where $\tau_n$ is a characteristic time scale of refractive index fluctuations over propagation path.

In order to derive an expression for the normalized cross-correlation function—the ultimate goal of this section—consider first the signal $P_1(t)$ that is registered by the photo-detector $PD_1$ in figure 1. In the case of a single-mode fiber, this signal is proportional to [10]

$$P_1(t) = \left|\int M_0(\mathbf{r})\psi_F(\mathbf{r}, t)\,\mathrm{d}^2\mathbf{r}\right|^2 \tag{2}$$

where the normalized function $M_0(\mathbf{r})$ describes the principal eigenmode of the single-mode fiber, and $\psi_F(\mathbf{r}, t)$ is the complex amplitude of the optical field that enters the fiber tip at the focal plane $F$ of the collimating lens $L_1$. Note that for a single-mode fiber, $M_0(\mathbf{r})$ is proportional to $\exp[-|\mathbf{r}|^2/w^2]$, where $w$ is the $1/e$ mode-field radius [10]. The complex amplitude of the optical field transmitted through the fiber tip is given by $A_F(\mathbf{r}) = c_0 M_0(\mathbf{r})$, where $c_0$ is a constant that

depends on the transmitted power. Correspondingly, $P_1(t)$ in (2) can be represented in the equivalent form

$$P_1(t) = \kappa_1 \left| \int A_F(\mathbf{r})\psi_F(\mathbf{r}, t)\, d^2\mathbf{r} \right|^2, \quad (3)$$

where $\kappa_1$ is a parameter that depends on both the transmitted power (through coefficient $c_0$) and photo-detector sensitivity. This expression can be further modified by considering complex amplitudes of the outgoing $A_B(\mathbf{r})$ and received $\psi_B(\mathbf{r}, t)$ optical fields in the lens $L_1$ rear plane (plane $B$ in figure 1). It can be easily shown (see below) that (3) can be rewritten as

$$P_1(t) = \kappa_1 \left| \int A_B(\mathbf{r})\psi_B(\mathbf{r}, t)\, d^2\mathbf{r} \right|^2. \quad (4)$$

As a next step, substitute $A_B(\mathbf{r})$ and $\psi_B(\mathbf{r}, t)$ in (4) by complex amplitudes $A(\mathbf{r}, z = 0)$ and $\psi(\mathbf{r}, z = 0, t)$ of optical fields at the collimating lens front plane (plane $z = 0$ in figure 1). Transformation of optical field complex amplitude after propagation through this lens can be described by the following complex transfer function, $W_1(\mathbf{r}) = a_1(\mathbf{r}) \exp[i\phi_1(\mathbf{r})]$, where $a_1(\mathbf{r})$ and $\phi_1(\mathbf{r})$ are the lens aperture and phase functions respectively. Taking into account that $A(\mathbf{r}, z = 0) = A_B(\mathbf{r})W_1(\mathbf{r})$ and $\psi_B(\mathbf{r}, t) = W_1(\mathbf{r})\psi(\mathbf{r}, z = 0, t)$, from (4) we obtain

$$P_1(t) = \kappa_1 \left| \int A(\mathbf{r}, z = 0)\psi(\mathbf{r}, z = 0, t)\, d^2\mathbf{r} \right|^2. \quad (5)$$

A similar expression can be derived for the signal $P_2(t)$ measured by the photo-detector $PD_2$ at the opposite end of the propagation path:

$$P_2(t) = \kappa_2 \left| \int A(\mathbf{r}, z = L)\psi(\mathbf{r}, z = L, t)\, d^2\mathbf{r} \right|^2 \quad (6)$$

where $\kappa_2$ is a parameter that depends on transmitted power and sensitivity of the transceiver $T_2$, and $L$ is the propagation distance.

For analysis of the correlation between the received signals $P_1(t)$ and $P_2(t)$ given by (5) and (6), consider the counter-propagating waves with complex amplitudes $A(\mathbf{r}, z, t)$ and $\psi(\mathbf{r}, z, t)$, where $0 \le z \le L$ is a coordinate collinear to propagation direction (optical axis) and $\mathbf{r} = \{x, y\}$ is coordinate vector in the plane orthogonal to the optical axis. For simplicity, we assume that the counter-propagating waves are monochromatic with identical wavelength $\lambda$. In the quasi-optical approximation, propagation of these waves can be described by the following system of parabolic equations [11]:

$$2ik\frac{\partial A(\mathbf{r}, z, t)}{\partial z} = \nabla_\perp^2 A(\mathbf{r}, z, t) + 2k^2 n_1(\mathbf{r}, z, t)A(\mathbf{r}, z, t), \quad (7)$$

$$-2ik\frac{\partial \psi(\mathbf{r}, z, t)}{\partial z} = \nabla_\perp^2 \psi(\mathbf{r}, z, t) + 2k^2 n_1(\mathbf{r}, z, t)\psi(\mathbf{r}, z, t), \quad (8)$$

where $\nabla_\perp^2 = \partial^2/\partial x^2 + \partial^2/\partial y^2$ is the Laplacian operator over the transversal coordinates, $n_1(\mathbf{r}, z, t)$ is a function describing the refractive index fluctuations, $k = k_0 n_0$, $k_0 = 2\pi/\lambda$ is the wavenumber, and $n_0$ is undisturbed value of the refractive index. Multiply (7) by $\psi(\mathbf{r}, z, t)$ and (8) by $A(\mathbf{r}, z, t)$ and subtract the second equation from the first. As a result we obtain

$$2ik\left[\psi\frac{\partial A}{\partial z} + A\frac{\partial \psi}{\partial z}\right] = \psi\nabla_\perp^2 A - A\nabla_\perp^2\psi. \quad (9)$$

Denote $\mathcal{C}$ the circle of infinite radius centered on $\mathbf{r} = \{0, 0\}$ and $\mathcal{S}$ the surface enclosed by $\mathcal{C}$. Integration of (9) over $\mathcal{S}$ gives

$$2ik\int_{\mathcal{S}} \frac{\partial(A\psi)}{\partial z}\, d^2\mathbf{r} = \int_{\mathcal{S}} [\psi\nabla_\perp^2 A - A\nabla_\perp^2\psi]\, d^2\mathbf{r}. \quad (10)$$

Applying Green's theorem, the right-hand side of (10) can be transformed into a contour integral

$$\frac{\partial}{\partial z}\left[\int A(\mathbf{r}, z)\psi(\mathbf{r}, z)\, d^2\mathbf{r}\right] = \frac{1}{2ik}\oint_{\mathcal{C}} [\psi\nabla_\perp A - A\nabla_\perp\psi]\cdot d\mathbf{r}. \quad (11)$$

By taking into account that the complex amplitudes $\psi(\mathbf{r}, z, t)$ and $A(\mathbf{r}, z, t)$ as well as their first derivatives vanish at infinity, we obtain the following conservation relationship for the overlapping integral between the counter-propagating wave complex amplitudes, also known as the interference metric [7, 12, 13]

$$J = \int A(\mathbf{r}, z)\psi(\mathbf{r}, z)\, d^2\mathbf{r} = \text{const}, \qquad 0 \le z \le L. \quad (12)$$

The interference metric (12) has thus the same value at both sides of the propagation path, that is

$$\int A(\mathbf{r}, z = 0)\psi(\mathbf{r}, z = 0)\, d^2\mathbf{r} = \int A(\mathbf{r}, z = L)\psi(\mathbf{r}, z = L)\, d^2\mathbf{r}. \quad (13)$$

Note that a relationship similar to (13) is fulfilled between the planes $F$ and $B$ of figure 1, which justifies the transition made earlier from (3) to (4). Using (5) and (6), expression (13) can be represented in the equivalent form $P_1(t)/\kappa_1 = P_2(t)/\kappa_2$ and correspondingly for the cross-correlation function in (1) we obtain:

$$\gamma_{12}(\tau) = \frac{\langle P_1(t)P_1(t+\tau)\rangle - \langle P_1(t)\rangle^2}{\langle P_1^2(t)\rangle - \langle P_1(t)\rangle^2}. \quad (14)$$

For the correlation coefficient $\gamma = \gamma_{12}(\tau = 0)$ from (14) follows:

$$\gamma = 1. \quad (15)$$

This suggests that in an optical link with finite aperture single-mode fiber transceivers the registered power signals are perfectly correlated, even in the presence of optical inhomegeneities along the propagation path. Note that (15) is also valid for the case of optical links based on single-mode fiber collimators with different aperture sizes. It is important to emphasize that in the derivation of (15), we did not use the reciprocity theorem but rather applied the conservation

property for the overlapping integral which is derived for the counter-propagating waves in parabolic approximation of the diffraction theory. Nevertheless the obtained result—perfect correlation of received power signals in the bidirectional link with single-mode fiber collimator transceivers—can be directly associated with the optical reciprocity principle and can be correspondingly referred to as reciprocity of received power signals.

## 3. Experimental analysis of received power signals correlation over a 7 km atmospheric propagation path

In this section, we present results of the experimental analysis of received power-signal correlations. The experiments were performed over a 7 km bidirectional atmospheric link. The notional schematic of the experimental setup is shown in figure 1. As laser transceivers, we used identical single-mode fiber collimators from Optonicus [14]. Each SMFC transceiver consisted of a collimating lens of 33 mm aperture diameter and 175 mm focal length and a single-mode fiber with 10 $\mu$m mode-field diameter whose tip was positioned at the collimating lens focal point. One SMFC transceiver was located on an optical bench next to a window on the fifth floor of the University of Dayton's College Park Center building at a height of 15 m. The second transceiver was placed on the rooftop of a 40 m-high building located 7 km away. The laser transceivers were carefully aligned by maximizing the averaged received power signals. This was performed by controlling the $x$- and $y$-position of the fiber tips with piezo-actuators. To minimize the impact of reflection of the outgoing beam from the fiber tip on the received power measurements, the SMFC transceivers were operated at slightly different wavelengths: 1555.75 and 1554.13 nm. These wavelengths correspond to the conventional fiber optics communication channels (channels 27 and 29) within the L-band of the 200 GHz ITU grid specification. Add-drop multiplexers were thus used instead of the beam splitters shown in figure 1 for the back-reflected light filtering. The received signals were synchronously detected by InGaAs detectors at both ends of the link. Turbulence strength was characterized by the refractive index structure constant $C_n^2$, which was measured with a scintillometer (*Scintec BLS* 2000). The received signals were simultaneously recorded in a set of experimental trials of 2.5 s duration, each with sampling rate of 5 kHz. The measurement synchronization was performed through an Ethernet link. An example of the received signal temporal dynamics at both ends of the propagation path during a typical experimental trial is shown in figure 2. The correlation coefficient $\gamma$ was computed by averaging the data acquired during 10 subsequent trials. The obtained value of the correlation coefficient $\gamma = 0.99$ with standard deviation not exceeding 1%, is in an exceptionally good agreement with the theoretical prediction described in section 2. The degree of signal correlation hardly changed with variation of turbulence strength and with the use of SMFC transceivers with significantly different aperture diameter. The latter was achieved by blocking a portion of one of the transceiver

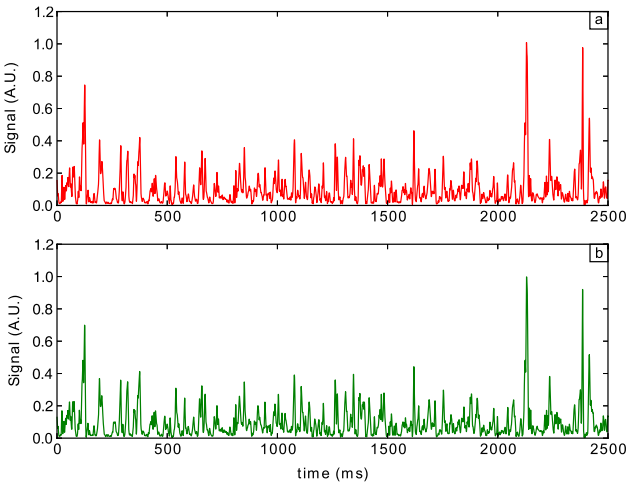


**Figure 2.** Temporal evolution of the received power signals $P_1(t)$ in (a) and $P_2(t)$ in (b) measured at opposite ends of a 7 km-long atmospheric propagation path with $C_n^2 = 5 \times 10^{-15}$ m$^{-2/3}$. The signals are presented in arbitrary units (AU). The computed correlation coefficient $\gamma$ between $P_1(t)$ and $P_2(t)$ is equal to 0.993.

apertures. Note that similar results indicating a high degree of correlation between received power signals were observed in a communication link between a 2 × 2 ground array of single-mode fiber based transceivers and a single-mode fiber based transceiver on-board an aircraft [15, 16].

The overlapping integral (interference metric) conservation law—the basis for ideal correlation of the received power signals—was derived in section 2 under the assumption that both SMFC transceivers operate with identical wavelengths. Nevertheless, as already mentioned in the experiments we used slightly different wavelengths. In order to evaluate the potential impact of wavelength mismatch as well as to analyze the correlation properties of received signals in optical links that utilize different types of optical transceivers we performed a set of numerical simulations that are described in section 4.

## 4. Received power-signal correlation in atmospheric turbulence conditions for different laser transceiver configurations: numerical simulations

In the numerical analysis we used the parameters of the experiments described above. The numerical simulation 1024 pixel × 1024 pixel grid corresponded to a 1.5 m × 1.5 m area in the plane orthogonal to the optical axis. Propagation of laser beams in a turbulent atmosphere was analyzed using numerical integration of the parabolic equations (7) and (8) with the standard split operator technique [17]. The turbulence-induced refractive index inhomogeneities along a 7 km-long propagation path were represented by a set of ten equidistantly located and statistically independent thin phase screens corresponding to Kolmogorov's refractive index fluctuation power spectrum [3, 11]. The phase screens were generated using the infinitely long phase screen technique [18]. We assumed that temporal fluctuations of the received power signals are solely caused by wind-induced

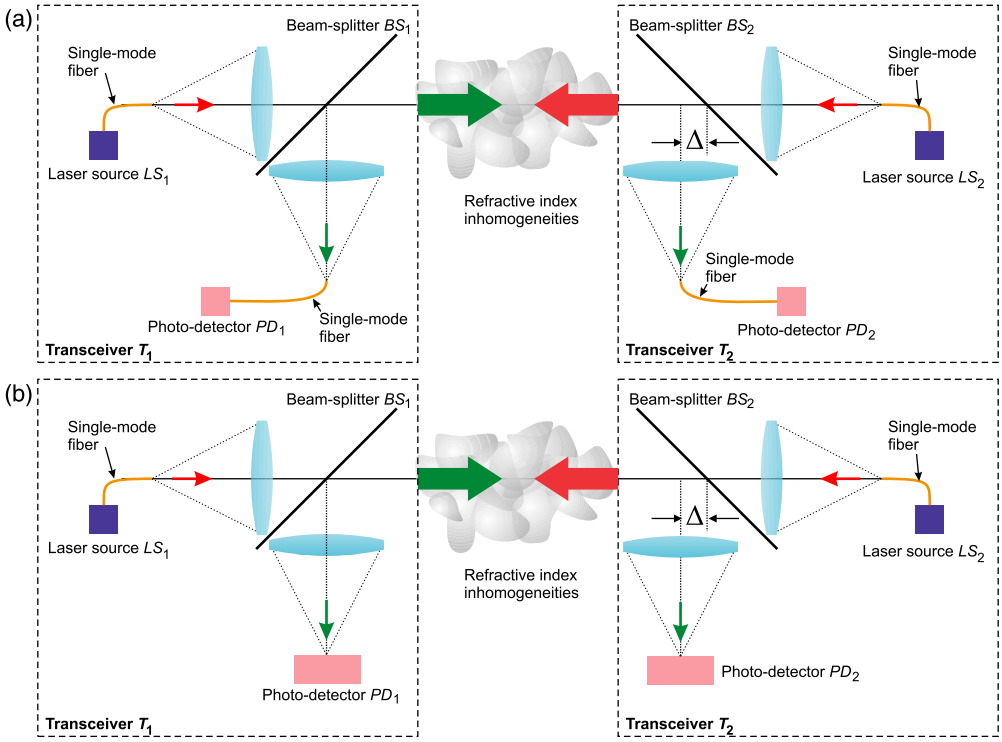


**Figure 3.** Notional schematics of optical links with bistatic transmitter–receiver configurations based on: (a) identical single-mode fiber collimators (SMFCs) as receivers and transmitters, and (b) SMFCs for laser beam transmission and power-in-the-bucket (PIB) receivers. In both schematics, the optical receivers on the right are misaligned by introducing a lateral shift Δ that results in a mismatch between the optical axes of the transmitted and received optical waves.

lateral translation of the entire air volume in the direction orthogonal to the optical axis (Taylor's frozen turbulence hypothesis). In the numerical analysis, a constant wind with 5 m $s^{-1}$ velocity was simulated using lateral translation of the phase screens. The functions $\psi(\mathbf{r}, z = 0, t)$ and $A(\mathbf{r}, z = L, t)$, obtained from numerical integration of (7) and (8), were used to compute the corresponding complex amplitudes at the SMFC transceiver focal planes as well as the power signals $P_1(t_i)$ and $P_2(t_i)$. Here $\{t_i, i = 1, \ldots, 10^5\}$ is a sequence of equidistant times of duration 29.3 s used to compute the correlation coefficient $\gamma$. The numerical simulations were performed for different turbulence conditions as characterized by the refractive index structure constant $C_n^2$ ranging from zero (no turbulence) to $C_n^2 = 10^{-14}$ $m^{-2/3}$ (strong turbulence). The numerical analysis results confirmed the predicted ideal correlation between received power signals. In all cases examined the deviation of the correlation coefficient $\gamma$ from the theoretical value $\gamma = 1$ did not exceed $10^{-9}$.

The numerical simulations also proved that the mismatch between wavelengths in the experiments described above results in negligible deviation of the correlation coefficient from the theoretical value. However, this deviation is no longer negligible for wider wavelength separation. Numerical simulations have shown that the correlation coefficient drops to $\gamma = 0.788$ when using the wavelengths 1064 and 1550 nm under strong turbulence conditions ($C_n^2 = 10^{-14}$ $m^{-2/3}$).

Consider now the counter-propagating optical settings in figure 3 which utilize separate transmitter and receiver apertures—the so-called bistatic transmitter–receiver configuration. This optical link type is commonly used in free-space optical communication applications. Note that both optical systems in figure 3 have identical single-mode fiber collimators (SMFC) transmitters but different type receivers. The optical receivers in figure 3(a) are based on single-mode fiber collimators (SMFC receivers), while in figure 3(b) each receiver is composed of a collimating lens and a wide-area photo-detector in its focal plane. This receiver, commonly referred to as power-in-the-bucket (PIB) receiver, measures the entire optical wave power that enters the collimating lens aperture.

Consider first the optical link shown figure 3(a). Note that with perfectly co-aligned receivers and transmitters this optical link is identical to the corresponding link with monostatic SMFC transceivers in figure 1. Correspondingly, the received power signals $P_1(t)$ and $P_2(t)$ in this system are perfectly correlated. Nevertheless, such perfect co-alignment is difficult or even impossible to achieve in practice. For example, to prevent energy losses of optical waves when passing beam splitters in figure 3, receiver and transmitter apertures are commonly mounted side by side with mutual displacement of optical axes a distance $\Delta > d$ apart of each other.

The question to ask is the following. How well is the correlation between the signals $P_1(t)$ and $P_2(t)$ preserved with a lateral shift of receiver and transmitter optical axes in figure 3? To answer this question, we performed numerical simulations using the parameters of the experimental setting described in section 3. The correlation coefficient between

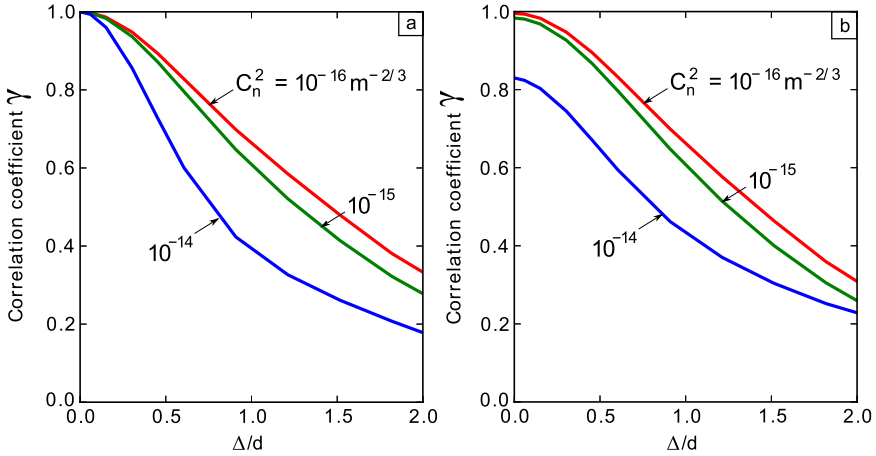


**Figure 4.** Dependences of the correlation coefficient $\gamma$ on the parameter $\Delta/d$ describing misalignment between the receiver and transmitter optical axis for: (a) optical link in figure 3(a), and (b) optical link in figure 3(b). Correlation coefficients are plotted for different values of the refractive index structure parameter $C_n^2$. In both cases the propagation path length is 7 km, the aperture diameters of the transmitters and receivers $d = 33$ mm and the wavelength is 1550 nm.

the power signals $P_1(t)$ and $P_2(t)$ was computed for different values of the misalignment parameter $\Delta$ that describes the distance between the optical axes of the transmitter and receiver apertures as shown in figure 3. Consider first the simulation results obtained for the optical configuration in figure 3(a). The corresponding dependences of the correlation coefficient $\gamma$ on the normalized distance $\Delta/d$, where $d$ is the aperture diameter, are presented in figure 4(a) for different turbulence conditions with $C_n^2$ ranging from $C_n^2 = 10^{-16}$ m$^{-2/3}$ (weak turbulence) to $C_n^2 = 10^{-14}$ m$^{-2/3}$ (strong turbulence). As the results show, when the separation distance $\Delta$ increases, the correlation coefficient gradually decreases. Furthermore, decorrelation of the received power signals occurs more dramatically as the turbulence strength increases. A 50% drop in correlation coefficient takes place with $\Delta = 0.75d$ for strong turbulence ($C_n^2 = 10^{-14}$ m$^{-2/3}$) and $\Delta = 1.45d$ in the case of relatively weak turbulence ($C_n^2 = 10^{-16}$ m$^{-2/3}$). This means that the location of the SMFC transceiver and receiver side by side may result in significant reduction of the power-signal correlation even in weak turbulence conditions.

Due to the presence of turbulence-induced phase aberrations, it is quite common that only a fraction of the entering receiver aperture power is coupled into the single-mode fiber. This may result in an insufficiently low signal-to-noise-ratio (SNR) in the measured power signal. The SNR can be increased by replacing the SMFC receivers with power-in-the-bucket (PIB) receivers.

Consider the impact of such a replacement on the received power-signal correlation. In numerical simulations of an optical link with PIB receivers in figure 3(b) we used parameters identical to the optical link with the SMFC receivers in figure 3(a). The dependences of the received power-signal correlation coefficient $\gamma$ on the misalignment parameter $\Delta/d$ are shown in figure 4(b) for different values of $C_n^2$. One can observe that the received power signals are only partially correlated even in the setting with perfectly aligned PIB receivers ($\Delta = 0$). As can be seen from figure 4(b) the correlation coefficient $\gamma = 0.996$ under weak turbulence ($C_n^2 = 10^{-16}$ m$^{-2/3}$) and drops to $\gamma = 0.83$ under strong turbulence conditions ($C_n^2 = 10^{-14}$ m$^{-2/3}$). With a lateral shift of the PIB receiver aperture, correlation gradually decreases. Similar to the optical configuration in figure 3(a), the lateral shift of the PIB receiver in figure 3(b) over the distance $\Delta > d$, which corresponds to side-by-side receiver and transmitter apertures, results in significant decorrelation of the power signals even in weak turbulence conditions.

It is quite common that in optical links with a bistatic transmitter–receiver configuration the aperture sizes of the receiver and transmitter are different. To analyze the impact of unequal aperture sizes on the correlation between received power signals, consider the bistatic optical links in figure 3 with perfectly aligned ($\Delta = 0$) but different size receiver and transmitter apertures. The dependences of the correlation coefficient $\gamma$ on the ratio $D/d$ between the receiver and transmitter aperture diameters are shown in figure 5(a) for the optical link based on SMFC transceivers (optical setting in figure 3(a)) in different turbulence conditions. These dependences have a well defined maximum $\gamma = 1$ at $D/d = 1$, that is, when receiver and transmitter aperture sizes are equal. As can be seen in figure 5(a), a mismatch between the receiver and transmitter aperture diameters results in decorrelation of the received power signals. This decorrelation is stronger in more severe turbulence conditions. Note that decorrelation of the received power signals occurs faster in the case when the receiver aperture diameters are smaller than the transmitters ($D < d$).

Consider now the dependences $\gamma(\eta)$ shown in figure 5(b) for the optical link with PIB receivers in the optical configuration of figure 3(b). In this case, the correlation coefficient curves have maxima at receiver aperture diameters $D < d$. With an increase in turbulence strength the maximum correlation between received power signals occurs with smaller size receivers.

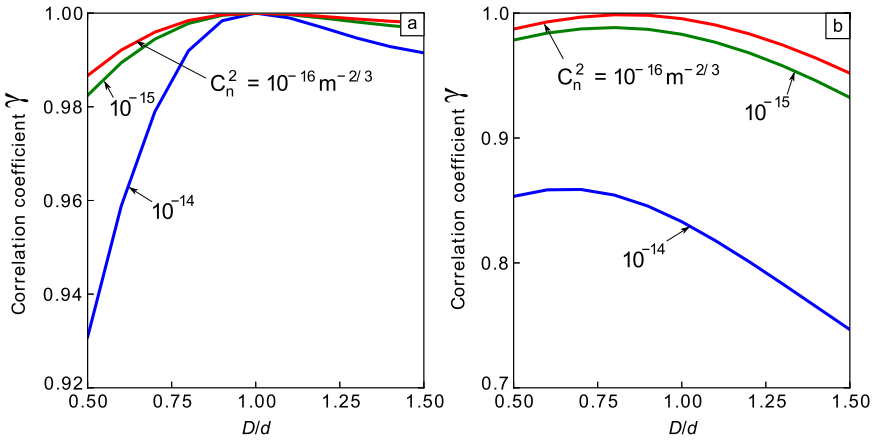


**Figure 5.** Dependences of the correlation coefficient $\gamma$ on the ratio of receiver and transmitter aperture diameters $D/d$ for: (a) optical link in figure 3(a), and (b) optical link in figure 3(b). Correlation coefficients are plotted for different values of the refractive index structure parameter $C_n^2$. The parameters are the same as in figure 4.

## 5. Concluding remarks on potential applications to laser communications

Correlation properties of power signals that are simultaneously measured at both ends of a bidirectional laser beam propagation path—the major objective of the study—can be utilized in different applications for mitigation of the negative impact of refractive index random inhomogeneities along the optical path of counter-propagating waves. One of the most obvious applications is related to the mitigation of atmospheric turbulence-induced signal fading in bidirectional laser communication links [19–21]. The optical signal fading mitigation problem inspired development of various techniques that can be subdivided into two major groups: optical (spatial, polarization, wavelength diversity [22], adaptive optics [21, 23, 24], etc) and signal/data processing (adaptive data rate [25], adaptive modulation and coding [26]) techniques. Although these techniques can provide some performance improvement of optical free-space communication systems, they nevertheless require either installation of complicated, bulky and expensive opto-electronic hardware (as in the case of adaptive optics and diversity based techniques), or setting up an additional link (optical or RF) for real-time channel-state information transmission (as in the case for adaptive data rate, and adaptive modulation and coding methods).

The strong correlation—observed in the experiments described here and confirmed through both theoretical analysis and numerical simulations—between received power signals in bidirectional optical links of different architectures opens attractive opportunities for the combination of optical and electronic (signal processing) tools for efficient mitigation of atmospheric turbulence effects. Indeed, with the nearly 100% correlation of received power signals that can be achieved in optical links based on single-mode fiber collimator transceivers, the data can be transmitted and received only during time intervals (fading-free time windows) when the received signal level exceeds a predefined threshold $P_{\rm thr}$ ($P_1 > P_{\rm thr}$ and $P_2 > P_{\rm thr}$) and can be buffered during fade times intervals (fading time windows) when $P_1 > P_{\rm thr}$ or $P_2 > P_{\rm thr}$. In the case of ideal correlation between received signals, these fading-free time windows occur at both ends of the communication link synchronously. This allows opening and closing the optical communication channel simultaneously for both laser communication transceivers without the need for sending back and forth channel-state (link availability) information between both transceivers. This turbulence-induced 'cooperation' between remotely located laser communication transceivers based on single-mode fiber collimators can also be used to enhance communication link security without encryption key distribution through the communication link. Different characteristics of simultaneously measured randomly varying power signals can be used to generate and/or change the encryption key at both ends of the communication link. For example, by setting a threshold value $P_{\rm thr}^{\rm key} > P_{\rm thr}$ for the received power signals and having identical devices that can generate a new encryption key at both ends of communication link each time when the received power signals exceed $P_{\rm thr}^{\rm key}$ one can use ideal correlation between independently measured received power signals to synchronously change the data encryption key at the same random set of times $\{t_j^{\rm thr}, j = 1, \ldots\}$ at both transceivers. Due to the rapid decay in the correlation coefficient with a lateral shift of the receiver aperture, as illustrated in figure 4(a), any attempt to use an optical receiver to intercept the data encryption key will fail even if the used threshold power level is known, since decorrelation of signals results in a different set of key change times. This turbulence-enhanced (physics based) communication link security provides an attractive alternative to technically complicated quantum communication techniques [27, 28].

## Acknowledgments

The authors thank Tom Tumolillo (Jr) and Jennifer Ricklin for helpful discussions. This work was supported in part by the US Air Force Office of Scientific Research MURI Contract no FA9550-12-1-0449 and by Cooperative

Agreement between the University of Dayton and Thales Research and Technology Corporation (France).

## References

[1] Kravtsov Y A 1993 *Appl. Opt.* **32** 2681–91
[2] Banakh V A and Mironov V L 1987 *LIDAR in a Turbulent Atmosphere* (Boston, MA: Artech House Publishers)
[3] Andrews L C and Phillips R L 1998 *Laser Beam Propagation Through Random Media* (Bellingham, WA: SPIE Press)
[4] Vorontsov M A and Kolosov V 2005 *J. Opt. Soc. Am.* A **22** 126–41
[5] Kravtsov Y A and Saichev A I 1982 *Sov. Phys.—Usp.* **25** 494–508
[6] Shapiro J H 1971 *J. Opt. Soc. Am.* **61** 492–5
[7] Vorontsov M A and Shmal'hauzen V I 1985 *Principles of Adaptive Optics* (Moscow: Nauka)
[8] Zel'Dovich B Ya, Pilipetsky N F and Shkunov V V 1985 *Principles of Phase Conjugation* (Berlin: Springer)
[9] Mandel L and Wolf E 1995 *Optical Coherence and Quantum Optics* (Cambridge: Cambridge University Press)
[10] Winzer P J and Leeb W R 1998 *Opt. Lett.* **23** 986–8
[11] Rytov S M, Kravtsov Y A and Tatarskii V I 1989 *Principles of Statistical Radiophysics 4, Wave Propagation Through Random Media* (Berlin: Springer)
[12] Arnaud J A 1976 *Beam and Fiber Optics* (New York: Academic)
[13] Vorontsov M A, Kolosov V V and Kohnle A 2007 *J. Opt. Soc. Am.* A **24** 1975–93
[14] www.optonicus.com
[15] Parenti R R, Michael S, Roth J M and Yarnall T M 2010 *Proc. SPIE* **7814** 78140Z
[16] Parenti R, Roth J and Shapiro J 2011 *Applications of Lasers for Sensing and Free Space Communications, OSA Technical Digest (CD)* Paper LTuD3
[17] Fleck J A, Morris J R and Feit M D 1977 *Appl. Phys.* **10** 129–60
[18] Vorontsov A M, Paramonov P V, Valley M T and Vorontsov M A 2007 *Waves Random Complex Media* **18** 91–108
[19] Parenti R R, Roth J M, Shapiro J H, Walther F G and Greco J A 2012 *Opt. Express* **20** 21635–44
[20] Minet J, Vorontsov M A, Polnau E and Dolfi D 2013 *Proc. of 2013 IEEE Aerospace Conference*
[21] Vorontsov M A, Carhart G, Gowens J W and Ricklin J C 2007 *US Patent Specification* 7,197,248
[22] Giggenbach D, Wilkerson B L, Henniger H and Perlot N 2006 *Proc. SPIE* **6304** 63041H
[23] Tyson R K 1996 *Appl. Opt.* **35** 3640–6
[24] Weyrauch T and Vorontsov M A 2004 *J. Opt. Fiber Commun. Rep.* **1** 355–79
[25] Levitt B K 1971 Variable-rate optical communications through the turbulent atmosphere *Tech. Rep.* Massachusetts Institute of Technology, Research Laboratory of Electronics
[26] Djordjevic I B 2010 *IEEE/OSA J. Opt. Commun. Netw.* **2** 221–9
[27] Gisin N, Ribordy G, Tittel W and Zbinden H 2002 *Rev. Mod. Phys.* **74** 145–95
[28] Gruneisen M T, Dymale R C and Stoltenberg K E 2011 *Proc. SPIE* **8189** 81891B